IMA Journal of Applied Mathematics (2019) Page 1 of 20
doi:10.1093/imamat/xxx000

Thermo-convective carbon sequestration in horizontal porous layers

K. GAUTAM
Department of Mathematics, Indian Institute of Technology-Hyderabad, Kandi, Sangareddy, Telangana, India 502285

AND

P.A.L. NARAYANA
Department of Mathematics, Indian Institute of Technology-Hyderabad, Kandi, Sangareddy, Telangana, India 502285

AND

A.A. HILL*
Department of Applied Sciences, University of the West of England, Bristol, UK
*Corresponding author: Antony.Hill@uwe.ac.uk

[Received on 13 March 2019]

This article explores the linear and nonlinear stability of double-diffusive density-driven convection in the context of carbon sequestration in deep saline aquifers. The anisotropy, due to the thermal and solutal diffusivities, is considered in a porous layer where the permeability is assumed to be layer dependent. Solute concentration is assumed to decay via a first-order chemical reaction. It is observed that varying the ratio of vertical to horizontal solutal and thermal diffusitivies does not significantly affect the behaviour of linear instability. This is in contrast to the nonlinear stability results. It is also observed that when the solute and thermal diffusion rates dominate the solute and thermal reaction rates, a change in the permeability has no significant effect on the onset of convection. However, when the solute reaction rate dominates the diffusion rate a change in permeability has a notable effect on the instability of the system. It is observed that the effects of geothermal gradient on the onset of convection are negligible as compared to the solutal effects induced by the diffusion and dissolution of CO_2 in deep saline aquifers.

Keywords: double-diffusive convection, anisotropic porous media, carbon sequestration, chemical reaction, stability theory

1. Introduction

The capture and geological storage of carbon dioxide (CO_2) in subsurface formations for the purpose of reducing anthropogenic emissions of CO_2 into the atmosphere is a highly promising technological advance, see Benson *et al.* (2008), Izgec *et al.* (2008), Nordbotten & Celia (2011) and Niem *et al.* (2017). The combustion of fossil fuels, mainly in power plants, is the biggest contributor to climate change through the increase of CO_2 in the atmosphere, IPCC (2013).

The storage capacity of storing CO_2 in underground deep saline aquifers has the potential for reducing greenhouse gas emissions while continuing the use of fossil fuels, see Metz *et al.* (2005), Holloway (2005). These saline aquifers are very large, unused and available in many parts of the world, see Gale (2004).

When supercritical CO_2 is injected above its critical point of pressure and temperature into deep

saline aquifers, dissolution of supercritical CO_2 in brine increases the density of CO_2-rich brine as compared to under-saturated brine, see Ennis-King & Paterson (2005), Ennis-King *et al.* (2005), Hassanzadeh *et al.* (2007) and Neufeld *et al.* (2010). As a result of density differences, the supercritical CO_2 migrates upwards and is trapped under impermeable cap-rock as a separate phase, see Bachu *et al.* (1994). Density-driven convection can occur, reducing the reservoir mixing time from thousand to hundred of years, see Harfash (2013), Ennis-King & Paterson (2005), Ennis-King *et al.* (2005), Kneafsey & Pruess (2010), Backhaus *et al.* (2011) and Slim *et al.* (2013).

The role of geochemical reactions on the dissolution of CO_2 in deep saline aquifers is largely unexplored despite it being able to contribute to a change in density, see Riaz *et al.* (2006) and Ward *et al.* (2014). Chemical interactions between carbon dioxide and brine are complex and can lead to a long-term stability and storage for CO_2 in subsurface formation. Many researchers have studied the effect of first and second order chemical reactions on the onset of convection for carbon dioxide sequestration in deep saline aquifers, see e.g. Ennis-King & Paterson (2007), Ghesmat *et al.* (2011), Andres & Cardoso (2011), Andres & Cardoso (2012), Kim & Choi (2014), Ward *et al.* (2014), Hill & Morad (2014), Kim & Kim (2015) and Kim & Wylock (2017).

Ennis-King & Paterson (2007) investigated the effect of a geochemical reaction on the convective mixing of CO_2 and showed that it accelerates the dissolution rate of CO_2 in geological formations. Kim & Choi (2014) analyzed the effect of a first-order chemical reaction in an isotropic porous media and suggested that the chemical reaction makes the system more stable and convective motion doesn't occur up to certain values of the Rayleigh and Damkohler number. Ward *et al.* (2014) studied stability analysis for convection in an isotropic porous media by using spectral and asymptotic methods where they assumed that the solute concentration decayed via the first order chemical reaction. They observed that the base flow undergoes numerous secondary bifurcations and there is an intricate network of mixing mode states.

The instability occurs due to the density difference between CO_2-rich brine and unsaturated brine. Modelling this physical phenomena is the main impetus behind the extensive research in this field and leads to the mathematical idealization of the stability of flows through the use of partial differential equations. Stability analysis of flows in porous medium helps to determine whether diffusive phenomena are stable or not. It has been of fundamental interest in various areas of science and engineering, such as geothermal engineering, physics and in carbon sequestration etc. For more details on the convection in porous media and applications, we refer to the book Nield & Bejan (2010) and the references therein.

Relevant to this article, Ennis-King & Paterson (2005) and Ennis-King *et al.* (2005) performed a stability analysis to investigate the role of the anisotropy in porous media at the onset of convection. Riaz *et al.* (2006) presented a linear stability analysis of density-driven miscible flow in a porous medium, based on the dominant mode of the self-similar diffusion operator to predict the critical time, the associated unstable wavenumber and a scaling relationship for the onset of convection. Xu *et al.* (2006) also studied the same problem and confirmed that linear theory gives a good understanding of the onset of convection. Hill & Morad (2014) studied the stability analysis in an anisotropic porous media in the presence of a first-order chemical reaction and have shown that anisotropy in porous media plays an important role in convective instabilities. They observed that when the diffusion rate is dominated by the reaction rate, varying the ratio of horizontal to vertical solute diffusivities does not significantly affect the behaviour of instabilities, while changes in the permeability has a substantial effect on the instability.

In the process of carbon dioxide sequestration in aquifers, the geothermal gradient (temperature) along with the concentration of CO_2 may contribute to the instability of the brine due to the increase in the density of brine. Javaheri *et al.* (2010) studied the effects of geothermal gradients on the stability

of double-diffusive natural convection induced by dissolution of CO_2 concentration and geothermal gradiant for a horizontal porous layer saturated with the brine in deep saline aquifers. They found that the natural geothermal gradient does not have a significant impact on the onset time of convective dissolution of CO_2 whereas concentration gradient has a significant effect.

Islam *et al.* (2013, 2014) investigated double-diffusive convection in two-dimensional brine saturated homogeneous and heterogeneous horizontal porous media subjected to the dissolution of CO_2 concentration and geothermal vertical gradients. Their results demonstrated that variation in temperature across the boundaries does not significantly affect the onset time of convection but the variation in the concentration played a significant role on the stability of the system. It was also observed that convection increases with increasing both Ra_S (solutal Rayleigh number) and heterogeneities and concentration of CO_2 increases over time with increasing the ratio of vertical to horizontal permeability in reservoirs. Islam *et al.* (2014a) analysed the effect of geochemical reaction rate of different orders on the density driven double-diffusive natural convection of CO_2 in brine saturated geothermal reservoir and showed that geothermal gradients play a minor role in storing the CO_2 in deep saline aquifers. However they may have an effect over long periods, and heterogeneity plays an important role in depositing CO_2.

Sabet *et al.* (2017) performed a linear stability analysis and direct numerical simulation to study the stability of double-diffusive convection in a horizontal porous media in the presence of variable viscosity. Their results showed that a higher Lewis number and viscosity contrast helps to increase the fluid mobility in the diffusive boundary layer.

In this work, we study the linear and nonlinear stability of double-diffusive convection in the context of carbon sequestration. Both thermal and solutal effects drive the convective instabilities in an anisotropic porous medium with constant solutal and thermal diffusivities and linearly layer-dependent permeability. Convective mixing and diffusion play an important role for trapping of CO_2 in formation brines in deep saline aquifers. The porosity (ϕ) here considered to be 0.30 for a typical reservoir, see Oldenburg & Pruess (1998). The eigenvalue problems obtained from both linear and non-linear stability theories is solved by the Chebyshev-tau method , which is a spectral technique coupled with QZ-algorithm, see Dongarra *et al.* (1996); Straughan & Walker (1996).

2. Mathematical formulation of the problem

Let us consider a fluid saturated porous layer Ω bounded by two horizontal infinite parallel plates separated by distance $2d$. Let $\Omega = \mathbb{R}^2 \times (-d, d)$ and $Oxyz$ be a Cartesian frame of reference. Assuming that the permeability varies in the vertical direction $k(z) = k_0 S(z)$, the flow governing Darcy equation under the Oberbeck-Boussinesq approximation can be written as

$$\frac{\mu}{k(z)}\mathbf{v} = -\nabla P - \mathbf{b}g\rho, \tag{2.1}$$

where $\mathbf{b} = (0,0,1)$ is the unit normal vector in the $z-$direction, $\mathbf{v}$ is the velocity vector, P is the pressure, g is the acceleration due to gravity, μ is the dynamic viscosity of the fluid, k_0 is the reference permeability and $S(z) = 1 + \lambda z/d$.

Here we consider the dissolution of a solute in Ω, where the solute undergoes a first-order chemical reaction, in which the solution density is increased due to the convective mixing. where the heat of the reaction is also modelled, as Ghesmat *et al.* (2011) and Islam *et al.* (2014a). Due to this effect, we are considering that there is a first-order reaction in solution by the natural geothermal temperature gradient. We denote the dissolved concentration in solution by C and temperature by T.

For a small change in density due to the temperature and concentration at a constant pressure, the

brine density is assumed to be linear with C and T. The density $\rho(T,C)$ is therefore given by

$$\rho(T,C) = \rho_0(1 - \alpha_T(T - T_0) + \alpha_C(C - C_0)),$$

where

$$\alpha_T = -\frac{1}{\rho_0}\left[\frac{\partial \rho}{\partial T}\right]_C \text{ and } \alpha_C = \frac{1}{\rho_0}\left[\frac{\partial \rho}{\partial C}\right]_T,$$

ρ_0, T_0 and C_0 are the reference values of density, temperature and concentration respectively. α_T and α_C are the coefficients for thermal and solutal expansions. Along with the equation for conservation of mass, the governing equations of the flow i.e. Darcy's law, concentration and heat transport are given by Islam *et al.* (2014a) and Ward *et al.* (2014)

$$\nabla \cdot \mathbf{v} = 0, \tag{2.2}$$

$$\frac{\mu}{k_0 s(z)}\mathbf{v} = -\nabla P - \mathbf{b}g\rho_0(1 - \alpha_t(T - T_0) + \alpha_c(C - C_0)), \tag{2.3}$$

$$\frac{1}{M}\frac{\partial T}{\partial t} + \mathbf{v}\cdot\nabla T = L_h\nabla'^2 T + L_v\frac{\partial^2 T}{\partial z^2} - \beta_T T, \tag{2.4}$$

$$\phi\frac{\partial C}{\partial t} + \mathbf{v}\cdot\nabla C = \phi k_h\nabla'^2 C + \phi k_v\frac{\partial^2 C}{\partial z^2} - \beta_C C, \tag{2.5}$$

where $\nabla'^2 = \frac{\partial^2}{\partial x^2} + \frac{\partial^2}{\partial y^2}$. In these equations, β_T and β_C are the reaction rate constants of temperature and solute, L_h and L_v are the constants horizontal and vertical thermal diffusivities and k_h and k_v are the constants horizontal and vertical solutal diffusivities.

$$(\rho_0 h)_m = (1-\phi)(\rho_0 h)_s + \phi(\rho_0 h_p)_f,$$

denotes the effective heat capacity of the matrix (fluid and rock), where h is the specific heat of the solid, h_p is the specific heat of the fluid at constant pressure. Subscripts s, f and m denote the solid, fluid and porous component of the medium, respectively. The coefficient M is the ratio of heat capacities defined by $M = (\rho_0 h_p)_f/(\rho_0 h)_m$.

We assume that the top and bottom boundaries are impermeable to the fluid flow, i.e. $\mathbf{v} = 0$ at $z = \pm d$. The upper boundary conditions for temperature T and solute concentration C are $C = C_0$, $T = T_0$ at $z = d$. The lower boundary conditions are assumed to be a no-flux boundary condition,

$$\frac{\partial C}{\partial z}\Big|_{z=-d} = 0, \qquad \frac{\partial T}{\partial z}\Big|_{z=-d} = 0.$$

Let $(\mathbf{v}_B, P_B, T_B, C_B)$ be the basic steady-state solution of the system $(2.2)-(2.5)$ for the motionless case, i.e. $\mathbf{v}_B = 0$. Utilizing the boundary conditions yields the temperature and concentration fields in the steady-state as

$$T_B(z) = \frac{T_0\cosh(\sqrt{d^2\beta_T/L_v}(z/d+1))}{\cosh(2\sqrt{d^2\beta_T/L_v})}, \tag{2.6}$$

$$C_B(z) = \frac{C_0\cosh(\sqrt{d^2\beta_C/\phi k_v}(z/d+1))}{\cosh(2\sqrt{d^2\beta_C\phi k_v})}. \tag{2.7}$$

To assess the stability of the system, we introduce a perturbation $(\mathbf{u},\pi,\theta,\Phi)$ to the basic steady-state solutions $(\mathbf{v}_B,P_B,T_B,C_B)$ such that $\mathbf{v}=\mathbf{v}_B+\mathbf{u},\ P=P_B+\pi,\ T=T_B+\theta,\ C=C_B+\Phi$, and governing equations are parametrized using the following scaling variables (* denotes dimensionless quantity)

$$t=\frac{d^2}{L_vM}t^*,\quad \mathbf{u}=\frac{L_v}{d}\mathbf{u}^*,\quad \pi=\frac{\mu L_v}{k_0}\pi^*,\quad \mathbf{x}=\mathbf{x}^*d,$$

$$\theta=\sqrt{\frac{\mu L_v\theta_0}{g\rho_0\alpha_t k_0 d}}\theta^*,\quad \Phi=\sqrt{\frac{\Phi_0\mu k_v}{g\rho_0\alpha_c k_0 d}}\Phi^*.$$

Substituting the perturbations and non-dimensionalised variables into the system $(2.2)-(2.5)$ and dropping the starred form, the system of dimensionless governing equations is given as

$$\frac{1}{f(z)}\mathbf{u}=-\nabla\pi+\mathbf{b}\sqrt{R_T}\theta-\mathbf{b}\frac{\sqrt{R_S}}{Le}\Phi, \tag{2.8}$$

$$\nabla\cdot\mathbf{u}=0, \tag{2.9}$$

$$\frac{\partial\theta}{\partial t}+\mathbf{u}\cdot\nabla\theta+R_T\sqrt{Da_T}M_1(z)w=\frac{\partial^2\theta}{\partial z^2}+\eta\nabla_1^2\theta-R_TDa_T\theta, \tag{2.10}$$

$$\hat{\phi}\frac{\partial\Phi}{\partial t}+\mathbf{u}\cdot\nabla\Phi+R_S\sqrt{Da_s}M_2(z)w=\frac{\phi}{Le}\left(\frac{\partial^2\Phi}{\partial z^2}+\xi\nabla_1^2\Phi-R_SDa_s\Phi\right), \tag{2.11}$$

subject to the perturbed dimensionless boundary conditions

$$\begin{gathered}\mathbf{u}=0,\quad \theta=0,\quad \Phi=0,\ \text{ at }\ z=1,\\ \mathbf{u}=0,\quad \frac{\partial\theta}{\partial z}=0,\quad \frac{\partial\Phi}{\partial z}=0,\ \text{ at }\ z=-1.\end{gathered} \tag{2.12}$$

Here $\mathbf{u}=(u_1,u_2,u_3)$ with $w=u_3$, $f(z)=1+\lambda z$ with $|\lambda|<1$ to ensure that $f(z)>0$,

$$M_1(z)=\frac{\sinh(\sqrt{R_TDa_T}(z+1))}{\cosh(2\sqrt{R_TDa_T})},\quad M_2(z)=\frac{\sinh(\sqrt{R_SDa_S}(z+1))}{\cosh(2\sqrt{R_SDa_S})}$$

and $\hat{\phi}=\phi M,\quad \xi=\frac{k_h}{k_v},\quad \eta=\frac{L_h}{L_v}$,

$$R_T=\frac{g\rho_0\alpha_t dk_0\theta_0}{\mu L_v},\quad R_S=\frac{g\rho_0\alpha_c dk_0\Phi_0}{\mu k_v},\quad Le=\frac{L_v}{k_v}$$

$$Da_T=\frac{\beta_T d\mu}{g\rho_0\alpha_t k_0\theta_0},\quad Da_S=\frac{\beta_c d\mu}{g\rho_0\alpha_c k_0\Phi_0\phi}$$

with R_T,R_S are the thermal, solute Rayleigh numbers and Da_T,Da_S are the thermal, solute Damkohler numbers, respectively. ξ is the ratio of horizontal to vertical solutal diffusivities and η is the ratio of horizontal to vertical thermal diffusivities. *Le* is the Lewis number.

We assume that the perturbations $(\mathbf{u},\pi,\theta,\Phi)$, defined on $(x,y,z)\in\Re^2\times[-1,1]$, are periodic functions in x and y directions of periods $2\pi/a_x, 2\pi/a_y$, respectively, with $a_x>0, a_y>0$ and the wave number $a=\sqrt{a_x^2+a_y^2}$. We will denote the periodicity cell by $\Omega_p=[0,2\pi/a_x]\times[0,2\pi/a_y]\times[-1,1]$.

3. Stability Analysis

It is crucial to assess the onset of convection (i.e. instability) after dissolution of carbon dioxide in brine to understand the processes occurring in the carbon dioxide sequestration in saline aquifers. To achieve this we perform two different stability analyses; namely a linear instability and a non-linear stability analysis (using the energy functional approach Straughan (2004, 2008)). Linear theory gives only sufficient conditions for instability, whereas non-linear analysis (via energy functionals) gives sufficient conditions for stability. The motivation for exploring both the linear and non-linear stability analyses is to identify the regions of sub-critical instabilities (if they exist) for the given flow governing parameter space.

3.1 *Linear instability analysis*

In order to investigate the linear instability analysis of the base flow, it is assumed that the perturbed velocities, pressure, concentration and temperature are small, such that the quadratic and higher order terms are neglected from the system $(8)-(11)$. As the resulting system of governing equations is linear and autonomous, we may seek solutions of the form

$$[u,v,w,\pi,\theta,\Phi] = [u(z),v(z),w(z),\pi(z),\theta(z),\Phi(z)]p_f(x,y)e^{\sigma t}, \tag{3.1}$$

where $p_f(x,y)$ is a plan-form which tiles the plane (x,y) with $\nabla_1^2 p_f(x,y) = -a^2 p_f(x,y)$ and $a^2 = a_x^2 + a_y^2$ is the overall wavenumber (a_x and a_y are the wave numbers in x and y directions). The plan-forms represent the horizontal shape of the convection cells formed at the onset of instability. These cells form a regular horizontal pattern tiling the (x,y) plane, where the wavenumber a is a measure of the width of the convection cell. Here $\sigma = \sigma_r + i\sigma_i$ is a growth rate parameter, where σ_r and σ_i are the real and imaginary parts of σ, respectively. $Re(\sigma) < 0$ corresponds to the case when the disturbance to base flow decays exponentially with time to zero which makes the system stable. $Re(\sigma) > 0$ corresponds to the case when disturbance grows exponentially with time leads to the system becomes unstable.

Letting $D = \frac{d}{dz}$ and taking double curl of the linearized version of Eq. (2.8), where the third component is chosen (i.e. $u_3 = w$ and the fact that $\mathbf{u}$ is solenoidal), we have the following set of governing equations for the linearized system

$$f(D^2 - a^2)w - \lambda Dw + \sqrt{R_T}a^2 f^2\theta - \frac{\sqrt{R_S}}{Le}a^2 f^2\Phi = 0, \tag{3.2}$$

$$(D^2 - a^2\eta)\theta - R_T Da_T\theta - R_T\sqrt{Da_T}M_1(z)w = \sigma\theta, \tag{3.3}$$

$$(D^2 - a^2\xi)\Phi - R_S Da_S\Phi - \left(\frac{Le}{\phi}\right)R_S\sqrt{Da_s}M_2(z)w = \sigma(MLe_v)\Phi, \tag{3.4}$$

subject to the boundary conditions

$$\begin{gathered} w = 0, \quad \theta = 0, \quad \Phi = 0 \text{ at } z = 1, \\ w = 0, \quad \frac{\partial\theta}{\partial z} = 0, \quad \frac{\partial\Phi}{\partial z} = 0 \text{ at } z = -1. \end{gathered} \tag{3.5}$$

The sixth-order system $(3.2)-(3.5)$ is solved by using the Chebyshev-tau method, which is a spectral technique coupled with the QZ-algorithm, see Dongarra *et al.* (1996) and Straughan & Walker (1996).

Numerical results for the linear theory will be presented Section 4. During the numerical simulation it is noted that for the given set of flow governing parameters the growth rate parameter σ is always found to be real at the onset of convection.

3.2 *Nonlinear stability analysis*

To achieve a global nonlinear stability bound in the stability measure $L^2(\Omega)$, we first remove the pressure term from Eq. (2.8), by taking double curl and using Eq. (2.9) to yield

$$\nabla^2 w - \frac{\lambda}{f}\frac{\partial w}{\partial z} - \sqrt{R_T} f \nabla_1^2 \theta + \frac{\sqrt{R_S}}{Le} f \nabla_1^2 \Phi = 0. \tag{3.6}$$

To proceed further with the global non-linear stability analysis, we use generalized energy functional technique by adopting the differential constraint approach, see Van Duijn *et al.* (2002), Pieters *et al.* (2006), Hill (2009), Capone *et al.* (2010), Capone *et al.* (2011), Hill & Morad (2014) and Gautam & Narayana (2019). Multiplying Eq. (10) by θ and Eq. (11) by Φ, respectively and integrating over domain Ω yields

$$\frac{d}{dt}\left(\frac{1}{2}\|\theta\|^2\right) = -\left\|\frac{\partial \theta}{\partial z}\right\|^2 - \eta\|\nabla_1\theta\|^2 - R_T Da_T \|\theta\|^2 - R_T\sqrt{Da_T}\langle M_1(z)w, \theta\rangle, \tag{3.7}$$

$$\frac{Le}{\phi}\frac{d}{dt}\left(\frac{\hat{\phi}}{2}\|\Phi\|^2\right) = -\left\|\frac{\partial \Phi}{\partial z}\right\|^2 - \xi\|\nabla_1\Phi\|^2 - R_S Da_S\|\Phi\|^2 - \left(\frac{Le}{\phi}\right) R_S\sqrt{Da_S}\langle M_2(z)w, \Phi\rangle, \tag{3.8}$$

where $\nabla_1 = \frac{\partial}{\partial x}\mathbf{i} + \frac{\partial}{\partial y}\mathbf{j}$ and $\langle .,. \rangle$ and $\|\cdot\|$ denote the inner product and norm on $L^2(\Omega)$ respectively. We now define the energy functional $E(t)$ as

$$E(t) = \frac{1}{2}\|\theta\|^2 + \tau\left(\frac{Le}{\phi}\right)\frac{\hat{\phi}}{2}\|\Phi\|^2, \tag{3.9}$$

where τ is a positive coupling parameter. Differentiating $E(t)$ with respect to t and using Eqs. (3.7) and (3.8), we derive the following identity

$$\frac{dE}{dt} = \mathscr{I} - \mathscr{D},$$

where

$$\mathscr{I} = -R_T\sqrt{Da_T}\langle M_1(z)w, \theta\rangle - \tau R_S\sqrt{Da_S}\langle M_2(z)w, \Phi\rangle,$$

$$\mathscr{D} = \left\|\frac{\partial \theta}{\partial z}\right\|^2 + \eta\|\nabla_1\theta\|^2 + R_T Da_T\|\theta\|^2 + \tau\left\|\frac{\partial \Phi}{\partial z}\right\|^2 + \tau\xi\|\nabla_1\Phi\|^2 + \tau R_S Da_S\|\Phi\|^2.$$

Defining the maximization problem

$$\frac{1}{R_E} = max_{\mathscr{H}}\left(\frac{\mathscr{I}}{\mathscr{D}}\right),$$

where $\mathscr{H}$ is the space of admissible perturbation solution to equations $(2.8) - (2.11)$ subject to constraint equation (3.6), we have

$$\frac{dE}{dt} \leqslant -\mathscr{D}\left(\frac{R_E - 1}{R_E}\right).$$

Utilising the Poincare inequality $2\pi^2\|u\|_{L^2(\Omega)} \leqslant \|\nabla u\|_{L^2(\Omega)}$, where Ω is an open connected locally compact Hausdorff space, it follows that $\mathscr{D} \geqslant rE$ for some positive constant r. Hence

$$\frac{dE}{dt} \leqslant -\left(\frac{R_E-1}{R_E}\right) rE.$$

After integration, we obtain

$$E(t) \leqslant E(0)e^{-\mathfrak{a}rt}, \tag{3.10}$$

where $\mathfrak{a} = \frac{R_E-1}{R_E}$. The inequality (3.10) gurantees that $E(t) \to 0$ exponentially as $t \to \infty$ for $R_E > 1$. Clearly, the decay of Φ and θ follows by the definition of $E(t)$. Using the Holder's and Young's inequalities in Eq.(8) yields

$$\frac{1}{1+\lambda}\|\mathbf{u}\|^2 \leqslant \frac{\Lambda}{2}\sqrt{R_T}\|\theta\|^2 + \frac{\chi}{2}\frac{\sqrt{R_S}}{Le}\|\Phi\|^2 + \frac{1}{2}\|\mathbf{u}\|^2\left(\frac{1}{\Lambda}+\frac{1}{\chi}\right),$$

for constants $\Lambda > 0$ and $\chi > 0$. Choosing $\Lambda = 2\sqrt{R_T}(1+\lambda)$ and $\chi = 2\frac{\sqrt{R_S}}{Le}(1+\lambda)$ gives

$$\|\mathbf{u}\|^2 \leqslant (1+\lambda)^2\left[Ra\|\theta\|^2 + \frac{Rs}{Le^2}\|\Phi\|^2\right]. \tag{3.11}$$

From Eqs. (3.9) and (3.11), it is observed that the decay of $\mathbf{u}$ follows from the decay of $E(t)$. Hence the system is stable for $R_E > 1$ in the stability measure $L^2(\Omega)$.

Introducing the Lagrange multiplier Ψ, such that

$$\Psi(\mathbf{x})\left(\nabla^2 w - \frac{\lambda}{f}\frac{\partial w}{\partial z} - \sqrt{R_T}f\nabla_1^2\theta + \frac{\sqrt{R_S}}{Le}f\nabla_1^2\Phi\right) = 0,$$

and using normal modes representation which is of the form as given in Eq. (3.1), the Euler-Lagrange equations for the maximization problem $1/R_E$ are

$$R_E\left(f(D^2-a^2)w - \lambda Dw + \sqrt{R_T}a^2f^2\theta - \frac{\sqrt{R_S}}{Le}a^2f^2\Phi\right) = 0, \tag{3.12}$$

$$R_E\left(f^2(D^2-a^2)\Psi - \lambda^2\Psi + \lambda fD\Psi - R_T\sqrt{Da_T}f^2M_1\theta - \tau\frac{Le}{\phi}f^2R_S\sqrt{Da_S}M_2\Phi\right) = 0, \tag{3.13}$$

$$R_E\left(R_T\sqrt{Da_T}M_1w - a^2f\sqrt{R_T}\Psi\right) = 2(D^2-a^2\eta)\theta - 2R_TDa_T\theta, \tag{3.14}$$

$$R_E\left(\frac{Le}{\phi}R_S\sqrt{Da_S}M_2w + \frac{\sqrt{R_S}}{\tau Le}a^2f\Psi\right) = 2(D^2-a^2\xi)\Psi - 2R_SDa_S\Psi, \tag{3.15}$$

with the corresponding boundary conditions

$$\begin{gathered} w=0, \quad \Psi=0, \quad \theta=0, \quad \Phi=0 \quad at\ z=1, \\ w=0, \quad \Psi=0, \quad \frac{\partial\theta}{\partial z}=0, \quad \frac{\partial\Phi}{\partial z}=0 \quad at\ z=-1. \end{gathered} \tag{3.16}$$

Eqs. (3.12) – (3.16) forms an eight-order eigenvalue problem for R_E, where global stability holds if $R_E > 1$ for all eigenvalues R_E (while maximizing over R_S, τ and minimizing over a^2). This eigenvalue problem is solved numerically by using the Chebyshev-tau method, which is a spectral technique coupled with QZ-algorithm, see Dongarra *et al.* (1996) and Straughan & Walker (1996).

4. Numerical results

In this section, the linear instability and non-linear energy theory numerical results are presented in relation to the physical variables in the system; namely the critical solutal Rayleigh number R_S, the thermal Rayleigh number R_T, the solutal Damkohler number Da_S, the thermal Damkohler number Da_T, the ratio of horizontal to vertical solutal and thermal diffusivities ξ and η and λ (such that $1+\lambda z$ describes the non-dimensional variable permeability varying in $z-$direction).

Figure 1 gives a visual representation of the linear instability thresholds with varying λ for different

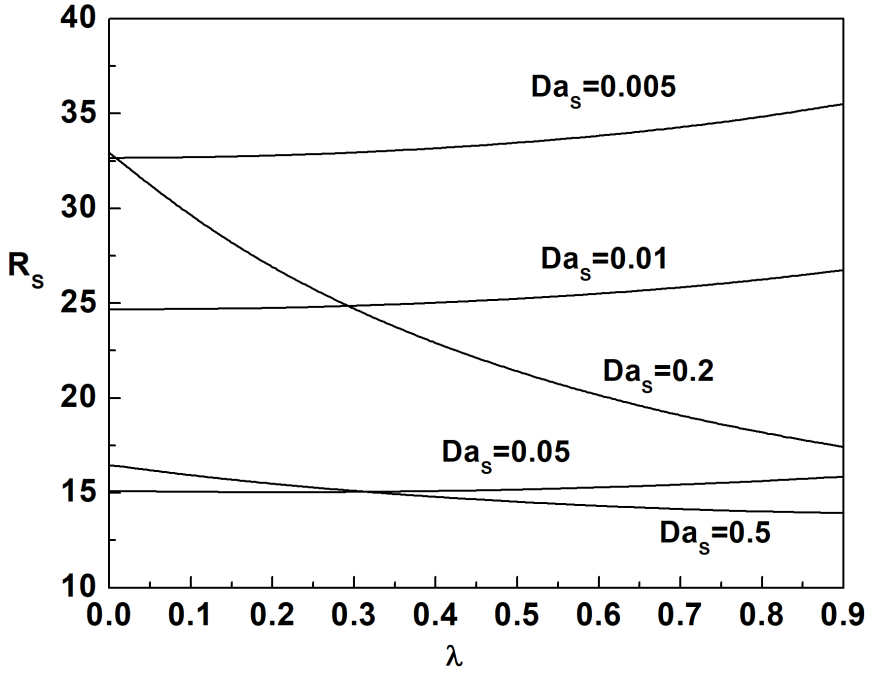

FIG. 1. Visual representation of linear instability threshold for $Da_S = 0.005, 0.01, 0.05, 0.2$ and 0.5 with critical solutal Rayleigh number R_S plotted against λ, where $R_T = 10, Da_T = 0.01, \eta = 1, \xi = 1, Le = 1$.

values of Da_S, respectively. From this figure it is noted that for the values of Da_S being between 0.005 to 0.05 (i.e. diffusion rate dominates solutal reaction rate), increasing the permeability λ in the vertical direction causes the system to become stable. In contrast to this, as the value of Da_S is further increased (i.e. when solutal reaction rate dominates diffusion rate, for values of $Da_S = 0.2$ and 0.5) a change in permeability λ causes system to become unstable. Therefore, there is a critical value of Da_S approximately 0.1 between two distinct behaviours for which λ becomes independent of the stability behaviour.

Figure 2 gives a visual representation of linear instability threshold with varying Le for different values of ξ. From Figure 2, it is clear that with increasing Le up to 0.9 an increase in ξ stabilizes the system. After $Le = 0.9$, there is no effect of ξ to be observed.

Figures 3*a* and 3*b* give a visual representation of the stability thresholds obtained in both linear and nonlinear theories with varying R_T for different values of η. Harfash (2013) pointed out that the two theories would contradict each other by providing entirely opposite phenomena on the stability of the

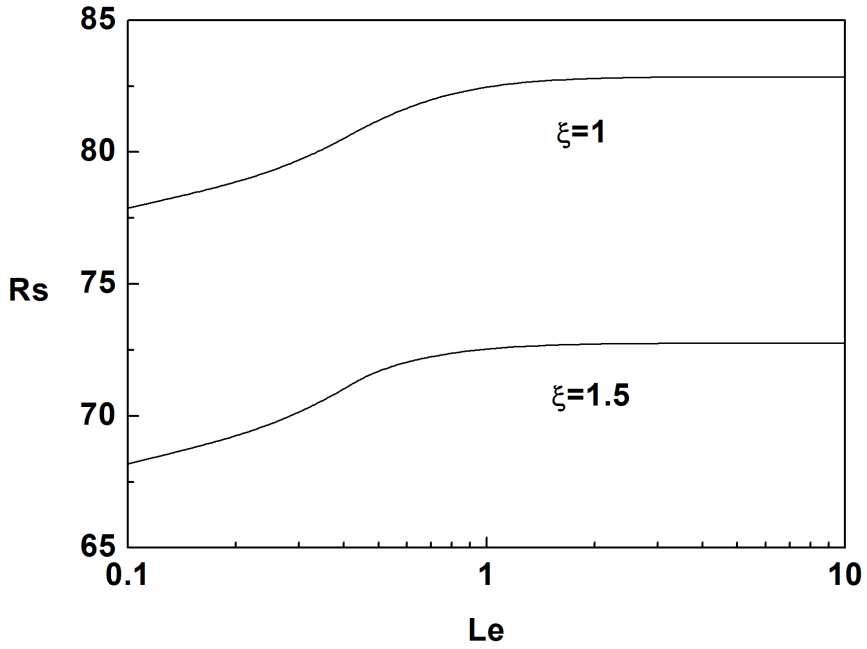

FIG. 2. Visual representation of linear instability threshold for $\xi = 0.5, 1.0,$ and1.5 with critical solutal Rayleigh number R_S plotted against Le, where $R_T = 10, Da_S = 0.001, Da_T = 0.01\lambda = 0.5, \eta = 0.01$.

system. Similar to Harfash (2013), in the present problem we observe that the nonlinear theory provides precisely the opposite phenomena observed in linear theory as shown in Figures 3*a* and 3*b*. From Figures 3*a*, 3*b*, it is noted that as the thermal Rayleigh number is increased in the linear theory the critical value of R_S is increased while in the case of nonlinear theory the same is reduced. This shows that R_T in linear theory has a strong stabilization affect whereas the same has a destabilization effect in the nonlinear theory.

Figure 4 gives the variation of critical R_S in both the linear and nonlinear theories against Da_S with varying ξ for fixed other flow governing parameters. It is clear from this Figure that the behaviour of neutral stability curves follow the similar trend in both linear and nonlinear theories for different values of ξ . It is observed that increasing ξ stabilizes the system. Destabilization is seen from $Da_S = 0.0001$ to $Da_S = 0.1$ and apparently stabilization afterwards.

When all the thermal parameters are fixed, the linear theory results obtained in the present paper strengthen the observations made by Hill and Morad (2014) for pure solutal convection. In particular, in spite of having quantitative effects on the stability of the system, the nonlinear stability neutral curves follow the similar trend as that of linear stability curves. The critical R_S in nonlinear theory is lesser than that of the critical R_S in linear theory yielding the regions of sub-critical instabilities. Furthermore it is observed that the region of sub-critical instabilities is narrowed from $Da_S = 0.0001$ to $Da_S = 0.1$ and this region is widened with further increase in Da_S.

Figure 5 gives a visual representation of the linear instability threshold with varying Da_T for different values of η, respectively. From Figure 5, it is observed that for fixed values of η with increasing the values of $Da_T = 0.0001$ to $Da_T = 0.08$ (i.e. when diffusion rate dominates thermal reaction rate)

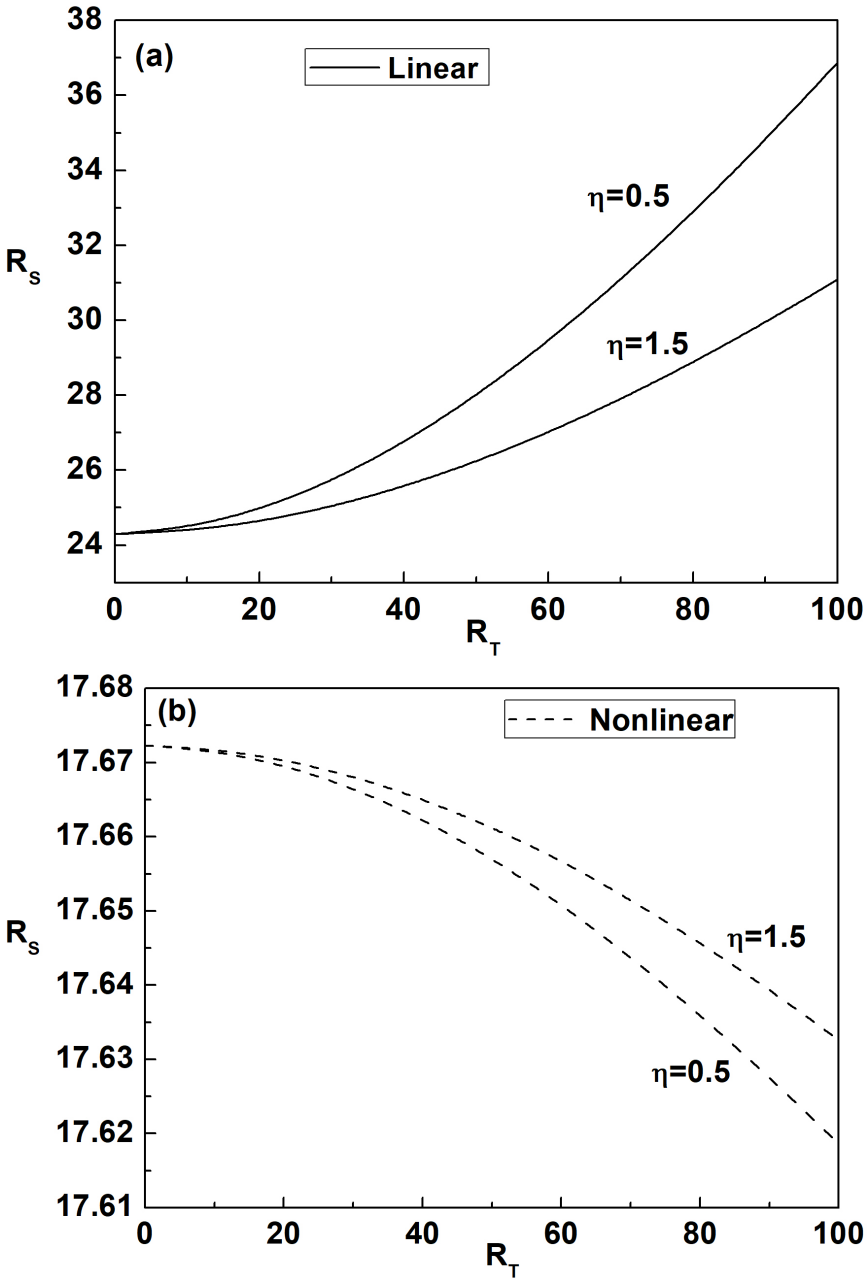

FIG. 3. Visual representation of linear instability threshold for $\xi = 0.5, 1.0,$ and1.5 with critical solutal Rayleigh number R_S plotted against Le, where $R_T = 10, Da_S = 0.001, Da_T = 0.01\lambda = 0.5, \eta = 0.01$.

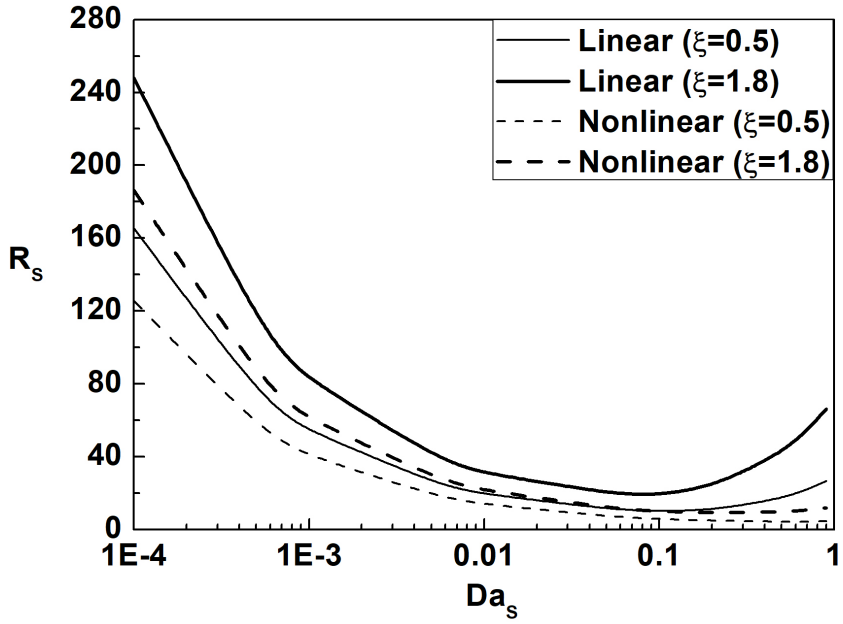

FIG. 4. Visual representation of linear (solid line) and nonlinear (dashed line) stability threshold for $\xi = 0.5, 1.8$ with critical solutal Rayleigh number R_S plotted against Da_S, where $R_T = 10, Da_T = 0.01, \eta = 1, \lambda = 0.2, Le = 1$.

stabilizes the system and further increasing (i.e. when thermal reaction rate dominates diffusion rate) destabilizes the system. The threshold for the onset of convection reduces with increasing the value η.

Figure 6 gives the variation of critical R_S in both the linear and nonlinear theories against Da_S with varying λ for fixed other flow governing parameters. From this Figure, it can be seen that there are potential regions for possible sub-critical instabilities. In region 1 (up to $Da_S = 0.08$), the region of sub-critical instabilities is decreased and the same is increased in region 2 where $Da_S > 0.08$. For mono-diffusive case it is observed by Hill and Morad (2014), that when the solutal diffusion rate dominates the solute reaction rate a change in the vertical permeability has no effect on the stability of the system. This is not true in the case of double diffusive convection with varying permeability in vertical direction. The threshold for the onset of convection in linear theory is increased with increasing λ up to $Da_S = 0.1$ and this threshold is decreased from $Da_S = 0.1$ onwards with an increase in λ. Similar behaviour is seen even in the nonlinear thresholds with marginal changes.

Figure 7 gives the variation of critical R_S in both the linear and nonlinear theories against Da_S with varying η for fixed other flow governing parameters. With increasing Da_S, the ratio between the horizontal and vertical thermal diffusivities (η) has no significant effect on the onset of convection. However in this case too, it is observed that the sub-critical instabilities would arise and follow the similar trend with Da_S as pointed out in the previous case. In conclusion, the ratio of horizontal to vertical thermal diffusivities (η) has no significant effect on the linear and nonlinear thresholds with the solutal Damkohler number.

Figures 8*a*, 8*b* give a visual representation of the stability thresholds obtained in both linear and nonlinear theories with varying λ for two different values of η and ξ, respectively. From these Figures it is observed that varying the vertical permeability of the medium stabilizes the system. From Figure 8*a* it is

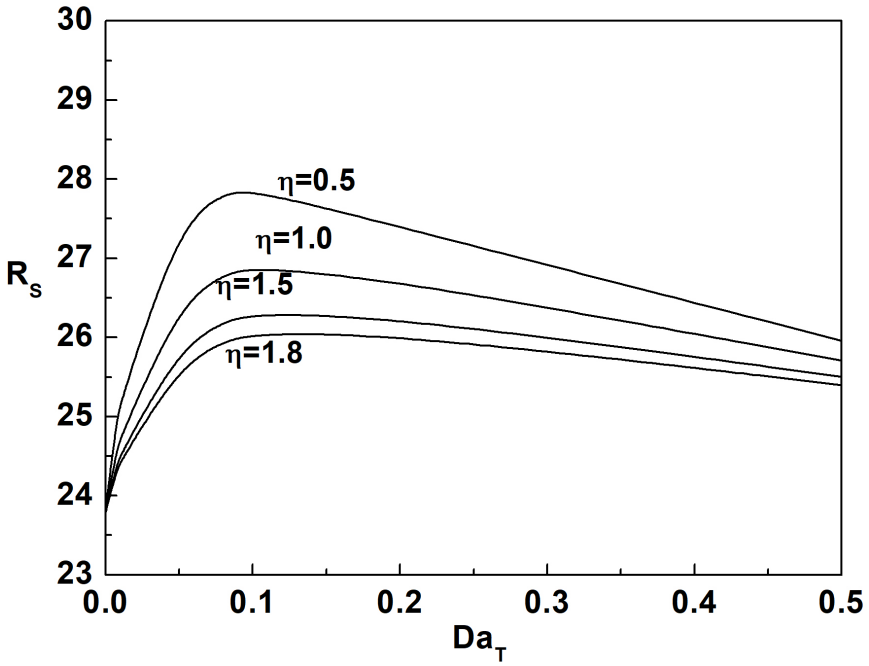

FIG. 5. Visual representation of linear instability threshold for $\eta = 0.5, 1.5$ with critical solutal Rayleigh number R_S plotted against Da_T, where $R_T = 10, Da_S = 0.01, \lambda = 0.5, \xi = 1, Le = 1$.

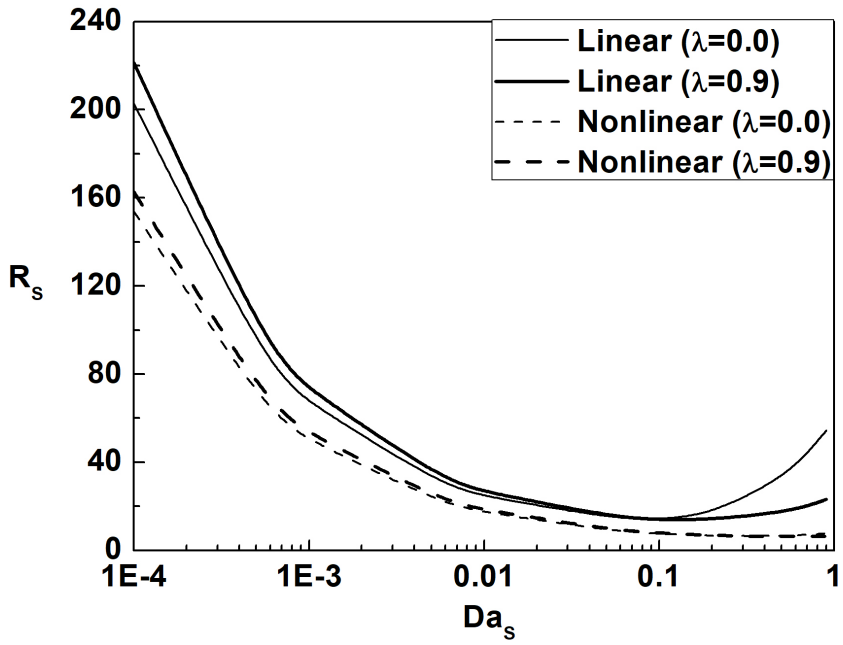

FIG. 6. Visual representation of linear (solid line) and nonlinear (dashed line) stability threshold for $\lambda = 0.0, 0.9$ with critical solutal Rayleigh number R_S plotted against Da_S, where $R_T = 10, Da_T = 0.01, \eta = 1, \xi = 1, Le = 1$.

clear that increasing η (i.e. horizontal thermal diffusivity dominates vertical thermal diffusivity) reduces the linear instability threshold for the onset while the nonlinear stability threshold is unaffected. The region of sub-critical instabilities exists between these two theories but this region is slightly reduced with η. In contrast to this, from Figure 8*b*, it is noted that increasing ξ (i.e. horizontal solutal diffusivity dominates vertical solutal diffusivity) has a significant effect on the thresholds obtained in both linear and nonlinear theories by stabilizing the system. However, the region of subcritical instabilities is enlarged with increasing ξ. From Figures $8(a)$ and $8(b)$, it is observed that the parameter ξ has precisely the opposite behaviour as compared to η for varying λ.

Figure 9 give a visual representation of the stability thresholds obtained in both linear and nonlinear theories with varying λ for different values of Da_T for fixed values of all solute parameters. From this Figure it is observed that for the fixed value of Da_T, increasing the vertical permeability of the medium stabilizes the system in both linear and nonlinear cases. When thermal reaction rate dominates diffusion rate (i.e. for higher values of Da_T) a change in the vertical permeability of the medium has a significant effect on the instability of a system. Furthermore it is noted that increasing the value of λ, the region of sub-critical instabilities is increased in both linear and non-linear theories.

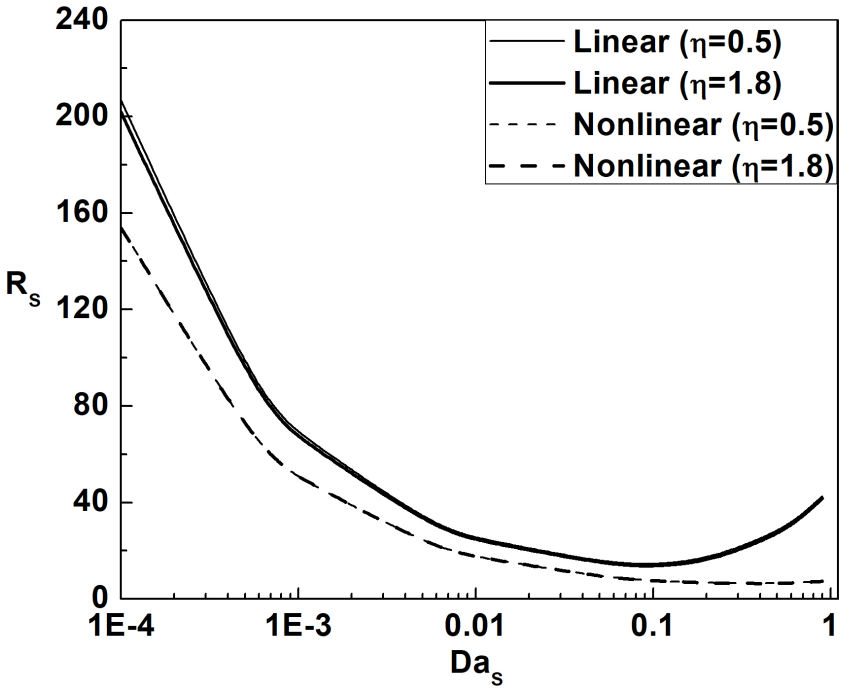

FIG. 7. Visual representation of linear (solid line) and nonlinear (dashed line) stability threshold for $\lambda = 0.0, 0.9$ with critical solutal Rayleigh number R_S plotted against Da_S, where $R_T = 10, Da_T = 0.01, \lambda = 0.2, \xi = 1, Le = 1$.

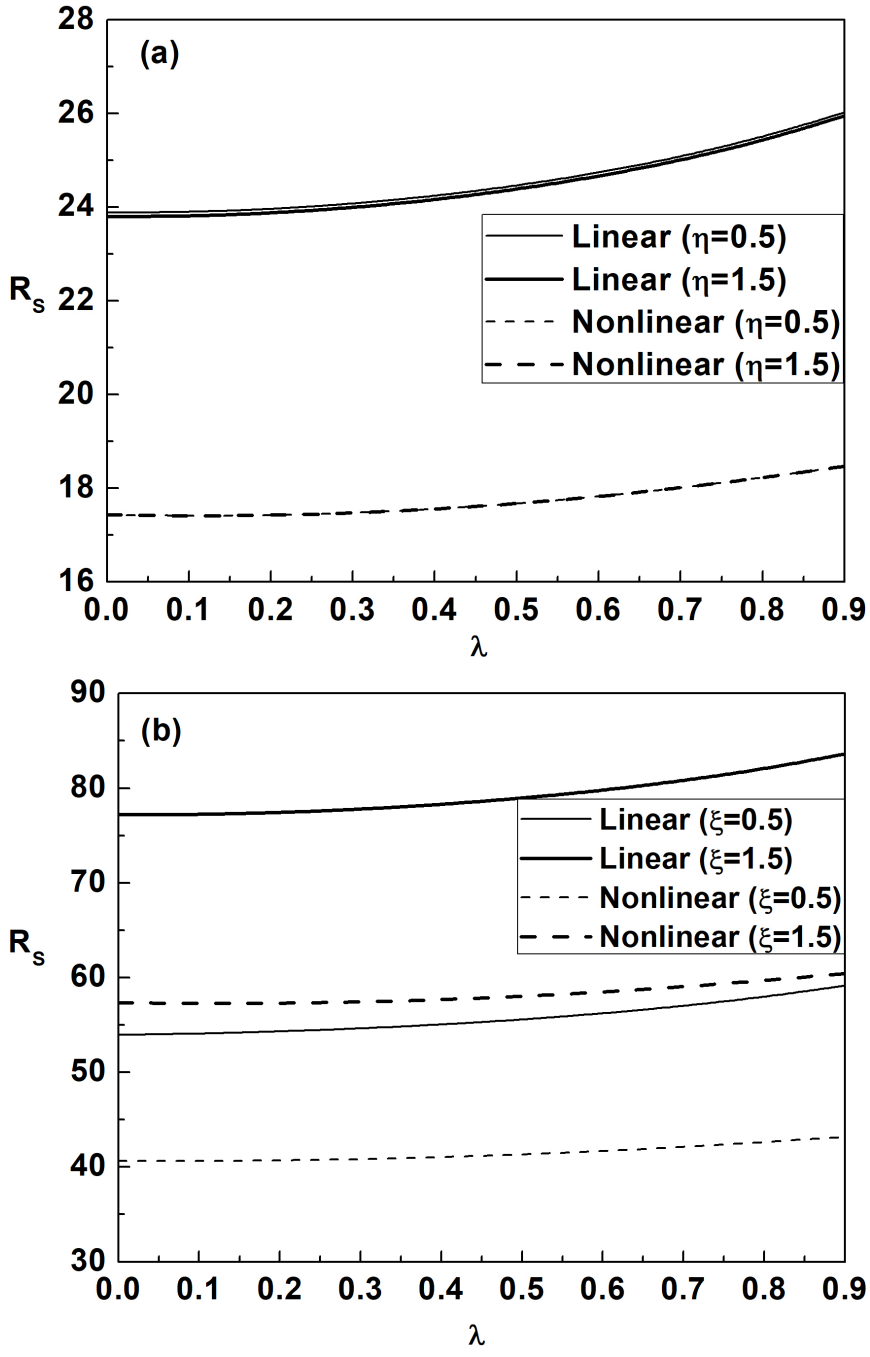

FIG. 8. (a), (b) : Visual representation of linear (solid line) and nonlinear (dashed line) stability threshold for $\eta = 0.5, 1.5$ and $\xi = 0.5, 1.5$ with critical solutal Rayleigh number R_S plotted against λ, where (a) $R_T = 10, Da_T = 0.001, Da_S = 0.01, \xi = 1, Le = 1$. (b) $R_T = 10, Da_T = 0.01, Da_S = 0.001, \eta = 1, Le = 1$.

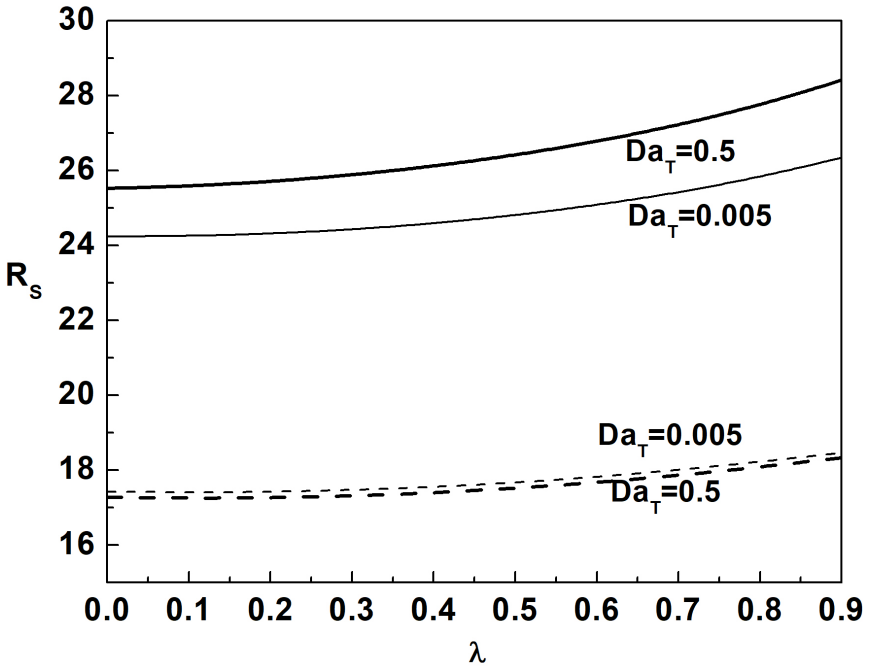

FIG. 9. Visual representation of linear (solid line) and nonlinear (dashed line) stability threshold for $Da_T = 0.005, 0.5$ with critical solutal Rayleigh number R_S plotted against λ, where $R_T = 10, Da_S = 0.01, \eta = 1, \xi = 1, Le = 1$.

5. Conclusion

In this work we have numerically investigated double-diffusive convection subject to vertical concentration and geothermal gradients in the context of carbon sequestration in deep saline aquifers. We performed linear and nonlinear stability analyses in an anisotropic porous media. In previous studies, Islam *et al.* (2013, 2014) and Javaheri *et al.* (2010), linear stability analyses were conducted subject to time dependent double-diffusive convection. In the present problem, we have analyzed the stability of the convective flow where concentration and temperature gradients are derived under a steady-state condition. Here, nonlinear theory was applied utilising an energy functional approach. The eigenvalue problem in both linear and nonlinear analyses are solved numerically by using the Chebyshev-tau method.

Based on our numerical results, we observed the following:

- in the linear theory, when the thermal diffusion rate dominates the reaction rate, the system is stabilized up to $Da_T = 0.08$ while destabilization is seen in the other case;
- R_T in linear theory corresponds to a strong stablization whereas the same has a destabilization effect in the nonlinear theory;
- the effect of permeability is observed to stabilize the system;
- when the thermal reaction rate dominates the diffusion rate, a change in permeability does not have a significant effect in both the linear and nonlinear stability analyses.

Acknowledgment

This work was supported through a research fellowship provided by the Council of Scientific and Industrial Research (CSIR), Government of India through the grant number "09/1001(0022)/2016-EMR-I" and the hospitality of Indian Institute of Technology Hyderabad.

REFERENCES

ANDRES, J.T.H. & CARDOSO, S.S. (2011) Onset of convection in a porous medium in the presence of chemical reaction. *Physical Review E*, **83**, 046312.

ANDRES, J.T.H. & CARDOSO, S.S. (2012) Convection and reaction in a diffusive boundary layer in a porous medium: Nonlinear dynamics. *Chaos: An Interdisciplinary Journal of Nonlinear Science*, **22**, 037113.

BACHU, S., GUNTER, W.D. & PERKINS, E.H. (1994) Aquifer disposal of CO_2: hydrodynamic and mineral trapping. *Energy Conversion and management*, **35**, 269–279.

BACKHAUS, S., TURITSYN, K. & ECKE, R.E. (2011) Convective instability and mass transport of diffusion layers in a Hele-Shaw geometry. *Physical review letters*, **106**, 104501.

BENSON, S.M. & COLE, D.R. (2008) CO_2 sequestration in deep sedimentary formations. *Elements*, **4**, 325–331.

CAPONE, F., GENTILE, M. & HILL, A.A. (2010) Penetrative convection via internal heating in anisotropic porous media. *Mechanics Research Communications*, **37**, 441–444.

CAPONE, F., GENTILE, M. & HILL, A.A. (2011) Double-diffusive penetrative convection simulated via internal heating in an anisotropic porous layer with throughflow. *International Journal of Heat and Mass Transfer*, **54**, 1622–1626.

DONGARRA, J.J., STRAUGHAN, B. & WALKER, D.W. (1996) Chebyshev tau-QZ algorithm methods for calculating spectra of hydrodynamic stability problems. *Applied Numerical Mathematics*, **22**, 399–434.

ENNIS-KING, J.P. & PATERSON, L. (2005) Role of convective mixing in the long-term storage of carbon dioxide in deep saline formations. *Spe Journal*, **10**, 349–356.

ENNIS-KING, J. & PATERSON, L. (2007) Coupling of geochemical reactions and convective mixing in the long-term geological storage of carbon dioxide. *International Journal of Greenhouse Gas Control*, **1**, 86–93.

ENNIS-KING, J.P., PRESTON, I. & PATERSON, L. (2005) Onset of convection in anisotropic porous media subject to a rapid change in boundary conditions. *Physics of Fluids*, **17**, 084107.

IPCC. (2013) Climate change 2013: *the physical science basis*. Geneva, Switzerland: Intergovernmental Panel on Climate Change.

GALE, J. (2004) Geological storage of CO_2: What do we know, where are the gaps and what more needs to be done?. *Energy*, **29**, 1329–1338.

GAUTAM, K. & NARAYANA, P.A.L. (2019) On the stability of carbon sequestration in horizontal porous layer. Preprint.

GHESMAT, K., HASSANZADEH, H. & ABEDI, J. (2011) The impact of geochemistry on convective mixing in a gravitationally unstable diffusive boundary layer in porous media: CO_2 storage in saline aquifers. *Journal of Fluid Mechanics*, **673**, 480–512.

HARFASH, A.J. (2013) Magnetic effect on instability and nonlinear stability of double-diffusive convection in a reacting fluid. *Continuum Mechanics and Thermodynamics*, **25**, 89–106.

HASSANZADEH, H., POOLADI-DARVISH, M. & KEITH, D.W. (2007) Scaling behavior of convective mixing, with application to geological storage of CO_2. *AIChE journal*, **53**, 1121–1131.

HILL, A.A. (2009) A differential constraint approach to obtain global stability for radiation-induced double-diffusive convection in a porous medium. *Mathematical methods in the applied sciences*, **32**, 914–921.

HILL, A.A. & MORAD, M.R. (2014) Convective stability of carbon sequestration in anisotropic porous media. *Proc. R. Soc. A*, **470**, 20140373.

HOLLOWAY, S. (2005) Underground sequestration of carbon dioxide—a viable greenhouse gas mitigation option. *Energy*, **30**, 2318–2333.

ISLAM, A., KORRANI, A.K.N., SEPEHRNOORI, K. & PATZEK, T. (2014a) Effects of geochemical reaction on double diffusive natural convection of CO_2 in brine saturated geothermal reservoir. *International Journal of Heat and Mass Transfer*, **77**, 519–528.

ISLAM, A.W., LASHGARI, H.R. & SEPHERNOORI, K. (2014) Double diffusive natural convection of CO_2 in a brine saturated geothermal reservoir: Study of non-modal growth of perturbations and heterogeneity effects. *Geothermics*, **51**, 325–336.

ISLAM, A.W., SHARIF, M.A. & CARLSON, E.S. (2013) Numerical investigation of double diffusive natural convection of CO_2 in a brine saturated geothermal reservoir. *Geothermics*, **48**, 101–111.

IZGEC, O., DEMIRAL, B., BERTIN, H. & AKIN, S. (2008) CO_2 injection into saline carbonate aquifer formations I. *Transport in Porous Media*, **72**, 1–24.

JAVAHERI, M., ABEDI, J. & HASSANZADEH, H. (2010) Linear stability analysis of double-diffusive convection in porous media, with application to geological storage of CO_2. *Transport in porous media*, **84**, 441–456.

KIM, M.C. & CHOI, C.K. (2014) Effect of first-order chemical reaction on gravitational instability in a porous medium. *Physical Review E* **90**, 053016.

KIM, M.C. & KIM, Y.H. (2015) The effect of chemical reaction on the onset of gravitational instabilities in a fluid saturated within a vertical Hele-Shaw cell: Theoretical and numerical studies. *Chemical Engineering Science*, **134**, 632–647.

KIM, M.C. & WYLOCK, C. (2017) Linear and nonlinear analyses of the effect of chemical reaction on the onset of buoyancy-driven instability in a CO_2 absorption process in a porous medium or Hele-Shaw cell. *The Canadian Journal of Chemical Engineering*, **95**, 589–604.

KNEAFSEY, T.J. & PRUESS, K. (2010) Laboratory flow experiments for visualizing carbon dioxide-induced, density-driven brine convection. *Transport in porous media*, **82**, 123–139.

METZ, B., DAVIDSON, O., DE CONINCK, H.C., LOOS, M. & MEYER, L.A. (2005) IPCC: *Intergovernmental Panel on Climate Change special report on carbon dioxide capture and storage*. Cambridge, UK: Cambridge University Press.

NIELD, D.A. (1968) Onset of thermohaline convection in a porous medium. *Water Resources Research*, **4**, 553–560.

NIELD, D.A. & BEJAN, A. (2010) *Convection in Porous Media*, third ed., Springer, New York.

NIEMI, A., BEAR, J. & BENSABAT, J. (2017) Geological Storage of CO_2 in Deep Saline Formations. Theory and Applications of Transport in Porous Media, vol. 29. New York, NY: Springer.

NEUFELD, J.A., HESSE, M.A., RIAZ, A., HALLWORTH, M.A., TCHELEPI, H.A. & HUPPERT, H.E. (2010) Convective dissolution of carbon dioxide in saline aquifers. *Geophysical research letters*, **37**.

NORDBOTTEN, J.M. & CELIA M.A. (2011) Geological storage of CO_2: modeling approaches for large-scale simulation. John Wiley and Sons, New York.

OLDENBURG, C.M. & PRUESS, K. (1998) Layered thermohaline convection in hypersaline geothermal systems. *Transport in Porous Media*, **33**, 29–63.

PIETERS, G.J.M. & VAN DUIJN, C.J. (2006) Transient growth in linearly stable gravity-driven flow in porous media. *European Journal of Mechanics-B/Fluids*, **25**, 83–94.

RIAZ, A., HESSE, M., TCHELEPI, H.A. & ORR, F.M. (2006) Onset of convection in a gravitationally unstable diffusive boundary layer in porous media. *Journal of Fluid Mechanics*, **548**, 87–111.

SABET, N., HASSANZADEH, H. & ABEDI, J. (2017) Stability of gravitationally unstable double diffusive transient boundary layers with variable viscosity in porous media. *AIChE Journal*, **63**, 2471–2482.

SLIM, A.C., BANDI, M.M., MILLER, J.C. & MAHADEVAN, L. (2013) Dissolution-driven convection in a Hele-Shaw cell. *Physics of Fluids*, **25**, 024101.

STRAUGHAN, B. (2004) *The energy method, stability, and nonlinear convection*, 2nd edn. Applied Mathematical Sciences, vol. 91. New York, NY: Springer.

STRAUGHAN, B. (2008) *Stability and wave motion in porous media*. Applied Mathematical Sciences, vol. 165. New York, NY: Springer.

STRAUGHAN, B. & WALKER, D.W. (1996) Two very accurate and efficient methods for computing eigenvalues and eigenfunctions in porous convection problems. *Journal of Computational Physics*, **127**, 128–141.

VAN DUIJN, C.J., PIETERS, G.J.M., WOODING, R.A. & VAN DER PLOEG, A. (2002) Stability criteria for the vertical boundary layer formed by throughflow near the surface of a porous medium. *Environmental Mechanics: Water, Mass and Energy Transfer in the Biosphere: The Philip Volume*, 155–169.

WARD, T.J., CLIFFE, K.A., JENSEN, O.E. & POWER, H. (2014) Dissolution-driven porous-medium convection in the presence of chemical reaction. *Journal of Fluid Mechanics*, **747**, 316–349.

XU, X., CHEN, S. & ZHANG, D. (2006) Convective stability analysis of the long-term storage of carbon dioxide in deep saline aquifers. *Advances in water resources*, **29**, 397–407.